A structurally tunable DNA-based extracellular matrix

Faisal A. Aldaye[1,2,*], **William T. Senapedis**[1], **Pamela A. Silver**[1,2,*], and **Jeffrey C. Way**[2]

[1] Department of Systems Biology, Harvard Medical School, 200 Longwood Ave., Boston, MA 02115, USA

[2] Wyss Institute for Biologically Inspired Engineering, Harvard University, 3 Blackfan Circle, Boston, MA 02115, USA

The construction of artificial matrices that mimic the structure and function of the naturally occurring extracellular matrix (ECM) is a central challenge for tissue engineering.[1] The difficulty lies in our inability to replicate the biophysical and chemical signaling effectors found in the ECM. Although polymeric hydrogels, nanofibrillar synthetic biomaterials, and PEG-based materials have been used for cell adhesion and proliferation,[2] there is a need for scaffolds that are structurally programmable. DNA nanotechnology uses base-pairing to generate predefined one-, two- and three-dimensional assemblies for the templated growth of materials, the organization of proteins and nanoparticles, and as platforms for diagnosis and delivery.[3] Here we combined the principles of DNA nanotechnology with protein engineering to generate a new class of DNA/protein extracellular matrices, and demonstrated their potential for cell adhesion and growth. The use of DNA means that our assemblies are inherently amenable to structural programming, which we demonstrated and used to fine-tune cell morphology, behavior, signaling, and transcription factor localization.

A DNA/protein-based matrix (**ECM$_{DP}$**) was constructed from a DNA ribbon (**ECM$_D$**) surface-functionalized with proteins (**ECM$_P$**) containing the RGD-domain of human fibronectin. This protein was selected because of its role in cellular adhesion, survival, proliferation and migration.[4] The structure of **ECM$_D$** was inspired by collagen. It is assembled from five DNA strands that form a 4-helix ribbon[3d] with overhangs (Scheme 1a), and analyzed using atomic force microscopy (AFM; Figure 1a).[11] **ECM$_P$** was expressed in *P. pastoris*, and contains a FN$_{III}$10 domain, a flexible (Gly$_4$Ser)$_3$ linker, a monomeric streptavidin domain for conjugation to 5′-biotin DNA, and a His$_6$ tag (Scheme 1b).[11] The 1:1 binding of **ECM$_P$** with DNA was confirmed using gel-shift assays.[11] Addition of **ECM$_P$** to **ECM$_D$** generated the DNA/protein matrix **ECM$_{DP}$** (Figure 2b).[11]

ECM$_{DP}$ promoted cell adhesion and migration. HeLa cervical cancer cells were used because of their well-characterized behavior,[5] and were found to attach onto **ECM$_{DP}$**-coated glass plates with 96% efficiency (Scheme 1c, Figure 1c, 1d).[11] Control experiments included using plates coated with **ECM$_D$**, **ECM$_P$**, unconjugated **ECM$_D$** and **ECM$_P$**, polylysine, or fibronectin.[6] These controls reveal that HeLa cells were incapable of effectively adhering onto **ECM$_D$** or **ECM$_P$**, unless assembled into **ECM$_{DP}$**, and that **ECM$_{DP}$** was as effective as polylysine or fibronectin for cell adhesion (Figure 1d).[11] The half-time of cell adhesion onto **ECM$_{DP}$** was 6 minutes, which was considerably faster than their rate of attachment onto polylysine or fibronectin (Figure 1e).[11] The force of adhesion was determined as a measure of detachment. We pretreated cells with the protein synthesis

faisal_aldaye@hms.harvard.edu, pamela_silver@hms.harvard.edu.

inhibitor cycloheximide to prevent deposition of cell-derived ECM proteins. As seen in Figure 1f, 90% of the cells remain attached to ECM_{DP} when a detachment force of 780 pN was applied,[11] which was considerably greater than the percentage of cells that remained attached to either polylysine or fibronectin. We also compared the effectiveness of ECM_{DP} to matrigel-coated surfaces, and found it to be comparable.[11] ECM_{DP} can thus be used as an effective extracellular matrix for cell seeding and attachment.

HeLa cells attached to $ECMD_{P}$ remained viable and migrated. We conducted flow cytometry experiments on cells stained with the apoptosis and necrosis fluorophores Annexin-V-EGFP and 7-AAD[7]. Only 4% of cells attached to ECM_{DP} stained positive for the apoptosis marker 48 hours after adhesion, and none were necrotic (Figure 1g).[11] In contrast, most of the cells attached to ECM_D died,[11] indicating that the protein element of ECM_{DP} was essential for cell survival. Motility was determined using a modified Oris™ cell-migration assay. HeLa cells moved on ECM_{DP} at a rate of 46µm/day (Figure 1h), which was slightly faster than their rates onto polylysine- or fibronectin-coated plates.[11] ECM_{DP} thus promotes cell survival and migration.

The structure of the ECM influence the cell's cytoskeletal arrangement and shape.[7] ECM_{DP} is fully double-stranded with a persistence length of 1.2 µm (i.e. length at which bending starts).[11] The incorporation of single-stranded domains should result in the formation of increasingly flexible assemblies that are structurally different (Figure 2a). $ECM_{DP}3$ and $ECM_{DP}10$ possess 3 and 10 base single-stranded regions and have persistence lengths of 0.95 and 0.32 µm, respectively (Figure 2b).[11] $ECM_{DP}3$ and $ECM_{DP}10$ are structurally more flexible than the fully double-stranded ECM_{DP}. Importantly, HeLa cells growing on EMC_{DP}, $ECM_{DP}3$ and $ECM_{DP}10$ were progressively more rounded (Figure 2c). These differences were confirmed by quantification of the substrate-bound integrin receptors (Figure 2d).[11] Focal adhesions form in response to increasing ECM stiffness.[7] Vinculin immunohistochemistry revealed a relative decrease in the number of assembled focal adhesions with increasing ECM flexibility.[11] We confirmed that the observed differences in cellular behavior is due to the structural changes resulting from the use of single-stranded DNA domains, and confirmed this engineering a set of fully double-stranded DNA assemblies analogues to ECD_{DP}, but with protein-to-protein distances that are identical to $ECM_{DP}3$ and $ECM_{DP}10$.[11] Collectively these results indicate that a profound cytoskeletal response can be achieved by controlling substrate structure. Using this, we proceeded to manipulate a number of integrin-mediated processes, such as the status of transduction proteins and the localization of intracellular transcription factors.

Focal adhesion kinase (FAK) is a signal transduction protein involved in cell development, migration, and in the regulation of the tumor suppressor p53.[10] FAK is phosphorylated in response to focal adhesion formation,[10] and can thus be fine-tuned as a function of ECM stiffness. As seen in Figure 2e, we were able to modulate the intracellular levels of p-FAK by modulating the degree of ECM single-stranded character.[11]

The integrin pathway can be used to activate the cytoplasmic versus nuclear localization of the transcription factor FOXO1a.[10] To test whether ECM stiffness could be used to fine-tune the intracellular localization levels of FOXO1a, we engineered a stable human osteosarcoma U2OS cell line expressing GFP-tagged FOXO1a fusions.[11] As seen in Figure 2f, by increasing the ECM's single-stranded character, we were able increase nuclear levels of FOXO1a.[11] We modulated FOXO1a localization, with potential consequences for cell differentiation, proliferation, longevity, and apoptosis.[9]

In summary, we constructed a new class of artificial extracellular matrices. Our approach involved the assembly of one-dimensional DNA ribbons decorated with cytoskeletal protein

elements. We demonstrated the potential of this material for *ex vivo* cellular scaffolding by showing that cells attach, survive and grow, and demonstrated its capacity for structural programmability by fine-tuning cell morphology, cytoskeletal organization, signal transduction, and transcription factor localization. The diversity and addressability of DNA nanostructures suggests that a multitude of artificial extracellular matrices could in principle be assembled using this approach. This contribution thus lays the groundwork for the modular construction of programmable ECMs to systematically study and replicate the naturally occurring extracellular niche.

Supplementary Material

Refer to Web version on PubMed Central for supplementary material.

Acknowledgments

References

1. (a) Ikada Y. J R Soc Interface. 2006; 3:589–601. [PubMed: 16971328] (b) Lutolf MP, Hubbell JA. Nature Biotech. 2005; 23:47–55.(c) Griffith LG, Naughton G. Science. 2002; 295:1009–1014. [PubMed: 11834815]

2. (a) Chan BP, Leong KW. Eur Spine J. 2008; 17:S467–S479.(b) Vasita R, Katti DS. Int J Nanomed. 2006; 1:15–30.(c) Lee KY, Mooney DJ. Chem Rev. 2001; 101:1869–1879. [PubMed: 11710233]

3. (a) Lo PK, Karam P, Aldaye FA, McLaughlin CK, Hamblin GD, Cosa G, Sleiman HF. Nature Chem. 2010; 2:319–328. [PubMed: 21124515] (b) Lin C, Liu Y, Yan H. Biochemistry. 2009; 48:1663–1674. [PubMed: 19199428] (c) Aldaye FA, Palmer AL, Sleiman HF. Science. 2008; 321:1795–1799. [PubMed: 18818351] (d) Yin P, Hariadi RF, Sahu S, Choi HMT, Park SH, LaBean TH, Reif JH. Science. 2008; 321:824–826. [PubMed: 18687961] (e) He Y, Tian Y, Ribbe AE, Mao C. J Am Chem Soc. 2006; 128:15978–15979. [PubMed: 17165718] (f) Um SH, Lee JB, Park N, Kwon SY, Umbach CC, Luo D. Nature Mater. 2006; 5:797–801. [PubMed: 16998469]

4. Yamada KM. Curr Opin Cell Biol. 1989; 1:956–963. [PubMed: 2534045]

5. Masters JR. Nature Rev Cancer. 2002; 2:315–319. [PubMed: 12001993]

6. We also conducted control experiments using unfunctionalized glass surfaces. See Supporting Information for details.

7. 7-AAD also stains cells in late apoptosis. We are thus unable to determine the exact ratio of cell death caused by apoptosis versus necrosis, and given that only 4% of cells die can conclude that **ECM$_{DP}$** is viable for cell growth.

8. (a) Discher DE, Mooney DJ, Zandstra PW. Science. 2009; 324:1673–1677. [PubMed: 19556500] (b) Discher DE, Janmey P, Wang YL. Science. 2005; 310:1139–1143. [PubMed: 16293750]

9. (a) Bershadskya AD, Ballestrema C, Carramusaa L, Zilbermana Y, Gilquinb B, Khochbinb S, Alexandrovac AY, Verkhovskyc AB, Shemeshd T, Kozlov MM. Eur J Cell Bio. 2006; 85:165–173. [PubMed: 16360240] (b) Wang YL. Sci STKE. 2007; 377:1–3.

10. (a) Hedrick SM. Nature Immunol. 2009; 10:1057–1063. [PubMed: 19701188] (b) Maiese K, Chong ZZ, Shang YC, Hou J. Med Res Rev. 2009; 29:395–418. [PubMed: 18985696]
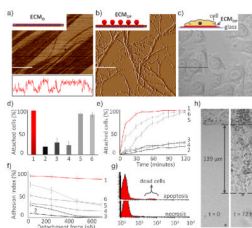
11. See Supporting Information for details.

Figure 1.
1–6 correspond to plates coated with **ECM$_{DP}$**, **ECM$_D$**, **ECM$_P$**, unconjugated **ECM$_D$** and **ECM$_P$**, polylysine, and fibronectin, respectively. (a) AFM characterization of **ECM$_D$**, with cross-sectional height analysis (lower panel). Bar 10 μm. (b) AFM characterization **of ECM$_{DP}$**. Bar 1 μm. (c) HeLa cells on **ECM$_{DP}$**-coated glass plates. Bar 15 μm. (d) Percentage of cells that attach onto **ECM$_{DP}$**-coated plates, and onto 2–6. (e) Rate of attachment. (f) Strength of attachment, as a function of detachment. (g) Viability of cells growing on **ECM$_{DP}$**. (h) Migration of HeLa cells growing on **ECM$_{DP}$**-coated plates.
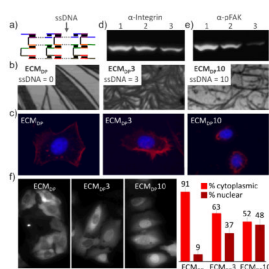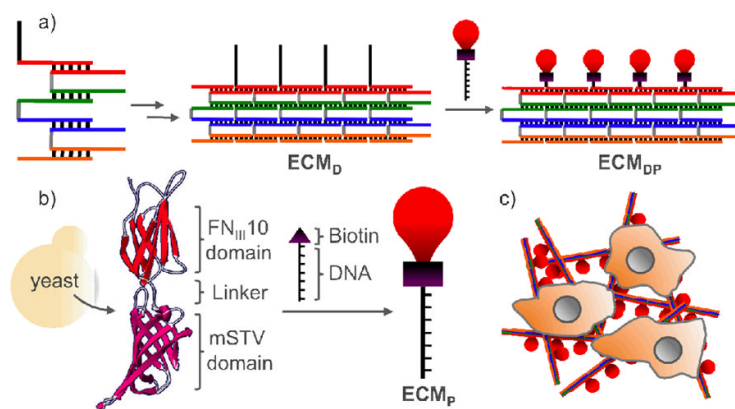
Figure 2.
(a) Single-stranded domains are used to fine-tune scaffold persistence length. (b) AFM analysis **ECM$_{DP}$**, **ECM$_{DP}$3**, **ECM$_{DP}$10**. (c) Cell morphology as a function of single-stranded character. Red, actin. Blue, nucleus. (d) Relative amounts of integrin receptors bound to **ECM$_{DP}$**, **ECM$_{DP}$3** and **ECM$_{DP}$10** (lanes 1–3, respectively). (e) Relative p-FAK expression levels as a function of **ECM$_{DP}$**, **ECM$_{DP}$3** and **ECM$_{DP}$10** (lanes 1–3, respectively). (f) GFP-FOXO1a localization as a function of scaffold persistence length. Statistics (right).

Scheme 1.